Low-Emittance Electron Bunches from a Laser-Plasma Accelerator Measured using Single-Shot X-Ray Spectroscopy

G. R. Plateau,[1,*] C. G. R. Geddes,[1] D. B. Thorn,[2,†] M. Chen,[1] C. Benedetti,[1] E. Esarey,[1] A. J. Gonsalves,[1] N. H. Matlis,[1] K. Nakamura,[1] C. B. Schroeder,[1] S. Shiraishi,[1] T. Sokollik,[1] J. van Tilborg,[1] Cs. Toth,[1] S. Trotsenko,[3,†] T. S. Kim,[1] M. Battaglia,[1,‡] Th. Stöhlker,[2,3,†] and W. P. Leemans[1,§]

[1]*Lawrence Berkeley National Laboratory, Berkeley, California 94720, USA*
[2]*ExtreMe Matter Institute EMMI, D-64291 Darmstadt, Germany*
[3]*Helmholtz-Institut Jena, D-07743 Jena, Germany*
(Received 15 April 2011; revised manuscript received 15 February 2012; published 10 August 2012)

X-ray spectroscopy is used to obtain single-shot information on electron beam emittance in a low-energy-spread 0.5 GeV-class laser-plasma accelerator. Measurements of betatron radiation from 2 to 20 keV used a CCD and single-photon counting techniques. By matching x-ray spectra to betatron radiation models, the electron bunch radius inside the plasma is estimated to be $\sim 0.1\ \mu$m. Combining this with simultaneous electron spectra, normalized transverse emittance is estimated to be as low as 0.1 mm mrad, consistent with three-dimensional particle-in-cell simulations. Correlations of the bunch radius with electron beam parameters are presented.

DOI: 10.1103/PhysRevLett.109.064802 PACS numbers: 41.75.Jv, 41.75.Ht, 52.38.Kd, 52.38.Ph

Laser-plasma accelerators (LPAs) [1,2] are tabletop-size devices that can produce temporally synchronized high-energy electron beams [3–6], THz [7,8], x-ray [9–11], and γ-ray radiation [12,13]. The electron density wave generated by an intense laser pulse ($> 10^{18}$ W/cm^2) propagating through a plasma can sustain gradients of hundreds of GV/m suitable for electron acceleration [2]. For sufficiently strong plasma waves, electrons from the bulk of the plasma can be self-trapped and accelerated to relativistic energies. To overcome the diffraction length of the laser and accelerate electrons to higher energies, the laser propagation distance can be increased by using both a plasma waveguide [4,6] and laser self-focusing [14]. Generation of high-quality 0.5–1 GeV electron bunches with few percent energy spreads has been demonstrated [6] using a capillary-discharge waveguide. Such electron bunches could be used to feed a free-electron laser (FEL) [15], providing a new generation of low-cost, compact sources. Experiments have so far demonstrated production of synchrotron radiation in the visible (0.6–1 μm) [16] and soft-x-ray (15–35 nm) [15] regimes using bunches with emittance estimated at $\sim$1 mm mrad. Decreasing the emittance is important to improve the performance of many applications of highly relativistic electron beams, such as accelerators for high-energy physics and drivers for x-ray FELs or Thomson γ-ray sources.

Recently, stable regimes of LPA operation in energy and divergence have been demonstrated [17–19], and single-shot high-resolution diagnostics of the emittance of GeV-scale bunches are needed to demonstrate the emittance and stability required for applications. Emittance measurements of low-energy ($\lesssim$ 120 MeV) electron bunches produced in LPAs have been reported using the "pepper-pot" technique [20–22]. Although single shot, these measurements had a limited resolution of $\sim$1 mm mrad and are difficult to apply to low-divergence high-energy beams. In addition, because the pepper-pot technique is a destructive detection method based on a sampling of the electron bunch, it prevents simultaneous use and diagnostics of the accelerator's electrons. An alternative method is to use the x-ray betatron radiation emitted by the electrons in the plasma as they accelerate [23,24] to characterize the electron bunch transverse size, which in combination with single-shot electron beam divergence measurements, provides an estimate of the normalized transverse emittance. In the bubble regime [2], the strong focusing fields of the ion bubble formed behind the driver laser pulse forces the electrons to undergo betatron motion and emit incoherent x-ray radiation. Previous x-ray betatron experiments [9–11] either had a limited resolution [25,26], relied on multishot spectral averaging [27], or induced the bunch radius from the spatial rather than the spectral x-ray distribution [28]. Simulations and theory indicate electron bunch radii and emittances may be at the 0.1 micron level, and measurements to date in LPAs have not resolved this scale.

In this Letter, high-resolution, single-shot x-ray spectroscopy measurements of betatron radiation are used to estimate the transverse emittance of electron bunches produced by a LPA. The far-field, on-axis radiation in the range of 2–20 keV was measured using a charge-coupled device (CCD) with a photon-counting technique [25]. The x-ray betatron spectrum shape allows inference of the beam radius σ_x because the shape is determined by the betatron strength parameter [23] $a_\beta \propto \sqrt{\gamma n_e} r_\beta$, where n_e is the plasma density and r_β is the amplitude of the betatron orbit of an electron. This parameter is analogous to the K parameter for conventional synchrotron or undulator radiation, but takes a somewhat different form for betatron radiation because the undulator is electrostatic instead of magnetic. As a_β increases, higher harmonics are emitted and as N_β decreases the harmonics broaden. For a beam with radius σ_x and a given momentum distribution, the spectrum is an incoherent sum over the spectra of the individual electrons. Different electrons have different a_β values, which typically blends the harmonics into a continuum whose shape is determined by σ_x and γ. Measured x-ray spectra were compared to theoretical spectra, indicating that the electron bunch radius σ_x inside the plasma was ~ 0.1 μm. Normalized transverse emittance was estimated to be as low as 0.1 mm mrad, consistent with simulations of self-trapping.

The experiments were performed on the LPA at the LOASIS facility of the Lawrence Berkeley National Laboratory. A schematic of the experimental setup is shown in Fig. 1. A 1.3 J, 24 fs rms Ti:Al_2O_3 laser pulse was focused to a 12 μm rms spot ($a_0 \simeq 1$) using an $f/25$ OAP. The laser was channeled in a 3.3 cm long, 250 μm diameter capillary discharge waveguide, filled with $0.4\text{–}1 \times 10^{19}$ e^-/cm^3 hydrogen plasma [6]. The electron bunch divergence and energy distribution were monitored using a magnetic dipole spectrometer [29]. The on-axis x-ray betatron radiation emitted by the electrons inside the plasma was collected using a back-illuminated Si CCD camera (Andor DY420-BR-DD) with 1024×256 pixels of 25 μm width. The active layer was 40 μm, and dead layer was 5 μm. A 1 MHz readout clock was used. The CCD was located 4.7 m from the LPA exit. The camera was coupled to the vacuum chamber with a window made of 0.1 μm Al, 14 μm polycarbonate, 18 μm Kapton, and 25 μm beryllium. An additional set of foils (33 μm Mylar, 73 μm polycarbonate, and 19 μm nitrocellulose) was used to avoid damaging or illuminating the CCD with the intense laser light, and it was verified that laser light did not affect the CCD. Broad-divergence bremsstrahlung x-ray background radiation was mitigated by separation of the camera from the accelerator area by a 60 cm-thick concrete wall. The low-divergence betatron x-ray beam propagated through an aperture in the wall to the CCD, which was encased by additional plastic and lead shielding.

The x-ray shadow of 680 μm diameter stainless-steel cross hairs located 1.7 m from the LPA exit was used to obtain an upper bound measurement of σ_x [11,25].

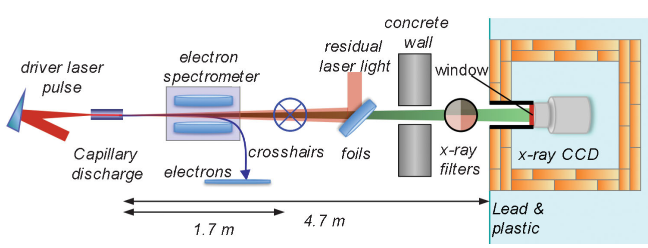

FIG. 1 (color). Setup for measurement of betatron x-rays from a LPA using a capillary-discharge waveguide plasma target.

From the edge sharpness of the shadow, integrated source size including shot-to-shot jitter in position was ≤ 4 $\mu\text{m} \simeq \lambda_p/4$. This measurement was limited by the single-pixel resolution of the CCD and the magnification ($2.7\times$). Because moving the cross hairs too close to the accelerator would result in ablation by the laser, higher resolution measurements relied on analysis of the spectra. Measurements of the x-ray divergence were not made due to the long coupling distance and resulting small solid angle subtended by the camera.

The x-ray CCD camera was calibrated for photon-counting spectroscopy [25,30,31] using a ^{55}Fe radioactive source. We consider both single-pixel absorption events where the deposited charge is confined to a single CCD pixel, which can be ensured by requiring that all surrounding pixels be below a threshold (here 5 counts) set above CCD noise (here 2 counts rms), and events where the charge cloud from a photon spreads over up to a 3×3 pixel group. The energy of the incident photon is determined from the charge in the pixel or pixel group. By generating a histogram of such events, single-shot x-ray spectra were calculated. Detection range was 2–20 keV (62–625 counts) with a resolution of 106 eV rms at 5.9 keV [25]. Accuracy was validated using synthetic data to verify that pileup (more than one photon hitting a pixel) did not affect data and by experimental comparison to filter spectra. A quadrant of filters (no filter, 10 μm Cu, 100 μm Al, 10 μm Cu, and 100 μm Al) was placed in front of the CCD, defining four subregions of the CCD. The spectrum of each of the three areas behind filters matched the convolution of the nonfiltered spectrum with the transfer function of the respective filters and detector response.

In a highly nonlinear wakefield such as that of the present experiments, electron beam σ_x can be inferred for a matched beam [2,23]. For a given energy $\sigma_x = \sigma_\theta(\lambda_p/\pi)\sqrt{\gamma/2}$, where σ_θ is the rms divergence of the beam and γ is the relativistic Lorentz factor. In the present experiments, the LPA typically produced quasimonoenergetic beams of $\sim$400 MeV energy with a rms energy spread of less than 5% and $\sim$1 mrad divergence from a plasma density of $5 \times 10^{18}/\text{cm}^3$, similar to the case in Refs. [6,18]. For such beams, the model yields $\sigma_x \sim 0.1$ μm, motivating high-resolution measurements to ascertain how close the experimental beams are to this matched limit. This corresponds to $a_\beta \sim 1$ for an electron at $r = \sigma_x$, where the first three odd harmonics are significant.

To infer σ_x from experimental betatron spectra, theoretical spectra must be calculated numerically, giving a set of spectral shapes that is compared to experiments to find the best match. While a critical energy can be calculated in the asymptotic limit, $a_\beta \gg 1$, this is not applicable for the parameters of the present experiments. Since the γ distribution is known from the magnetic spectrometer, σ_x is the free parameter determining the spectral shape. The height of the spectrum is determined by the bunch charge Q and the number of betatron oscillations N_β the electrons execute, at wavelength λ_β and over the radiation length $L_{\rm rad} = N_\beta \times \lambda_\beta$. These parameters do not significantly affect spectral shape for an emittance-matched beam. Hence, the matching of theory and experiment can be first conducted on the spectral shape ignoring amplitude, which allows inference of σ_x. Since the charge is known from the magnetic spectrometer, the observed spectral amplitude allows inference of $L_{\rm rad}$. Because the CCD did not measure the radiation distribution in the present experiments, the angular distribution of radiation is the principal source of error in the fitting of experiments to theory. For this reason, spectra on axis were calculated using analytical formulas of betatron theory [23] and spectra integrated over emission angle using numerical integration of electron trajectories using the code VDSR [32]. In general, the highest energy emission is on axis, and as a result angle-integrated spectra may return a larger best-fit radius than on axis.

X-ray betatron spectra were modeled and compared to the measured spectrum to extract σ_x. Figure 2 shows a single-shot detected x-ray betatron spectrum (which is uncorrected and includes camera and filter response) from an electron bunch of 463 MeV ($\gamma \sim 900$), with 2.8% rms energy spread and $\sigma_\theta = 1.2$ mrad rms divergence, accelerated in a plasma of density $5 \pm 2 \times 10^{18}$ e^-/cm^3. Good agreement between the experiment and the angle-integrated theoretical spectra, convolved with camera and filter response, is obtained for $\sigma_x = 0.1$ μm, where the χ^2/ndf statistic is 0.8. For $\sigma_x = 0.03$ μm and $\sigma_x = 0.3$ μm, calculated angle-integrated spectra diverge

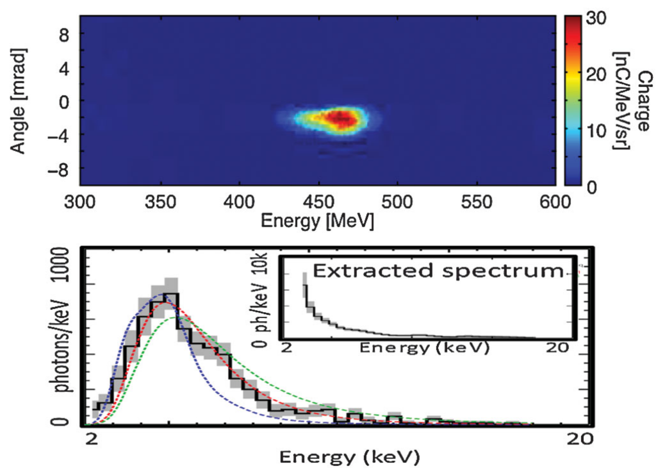

FIG. 2 (color). Simultaneous single-shot electron energy distribution (top) and detected x-ray betatron spectrum (bottom). The detected x-ray spectrum (black; shaded region shows 1-σ uncertainty) is matched by the angle-integrated theoretical spectrum, convolved with filters/detector response, for $\sigma_x = 0.1$ μm (red). Models for $\sigma_x = 0.03$ (blue) or 0.3 μm (green) diverge from the data. Inset shows x-ray spectrum of the source, with instrument response extracted.

visibly from the data and the χ^2 statistic indicates these can be excluded at the 98% confidence level. Included in the displayed error bars are shot noise and uncertainty in plasma density, CCD dead layer thickness, and analysis thresholds. On-axis calculations returned $\sigma_x = 0.1$ μm ($\pm$ 0.05 μm), which agrees within the confidence level with the angle-integrated spectra. Including effects of acceleration during the emission process (i.e., $\gamma(z) \neq$ const) did not significantly affect the fit, since radiation is dominated by the high-energy portion of the trajectory. Simulations also indicate that narrow energy spread electron beams are only present near peak energy.

Adiabatic expansion of the bunch in the plasma down ramp [21] is weak for these parameters due to a short ramp of only $\sim 3 \times \lambda_\beta$ and strong depletion of the laser energy after propagating through the 3.3 cm plasma channel, which weakens the wake in the ramp. Space charge effects are also weak for the high-energy beam. Hence, the beam does not evolve on exiting the plasma, and σ_θ observed on the spectrometer is accurate.

The σ_x value obtained from the betatron spectra is in agreement with the matched beam radius for the observed σ_θ, $\sigma_{x(\rm match)} = 0.1^{+0.05}_{-0.02}$ μm. This indicates the beam is close to the matched condition in the plasma structure.

Using the charge on the electron spectrometer, $Q \sim 0.4$ pC, we fit the experimental x-ray spectrum height to the on-axis radiation calculation, giving a lower limit on the radiation length over which electrons propagated while emitting >2 keV betatron x-rays, $L_{\rm rad} = 400 \pm 200$ μm. This is less than but of the order of the acceleration length L_ϕ, compatible with the distance the electrons are expected to be at high energy. Only a lower limit is available because the CCD does not collect the full radiation envelope.

Shot-to-shot fluctuation in beam performance was used to characterize dependence of σ_x on divergence by operating near the threshold for self-trapping, where beam parameters fluctuate sensitively with laser amplitude [4,6]. Fits were conducted for normalized spectra binned by electron beam divergence. This provided adequate statistics for fitting, required since not all single shots are adequate due to fluctuations in charge and in photon distribution on the CCD (only isolated hits are accepted). To obtain a consistent data set we considered shots that had at least 100 single-pixel photon hits, energies between 200 and 500 MeV, and energy spread of less than 5% rms. These shots were 20% of the data set and averaged 2.5 pC, which is far from the beam loading limit on charge. Mean energies for all bins were within 20 MeV ($< 1\sigma$) of 340 MeV, allowing independent analysis of divergence effects. Variation of inferred σ_x with electron beam divergence is consistent with the expected linear dependency (Fig. 3), and the best fits are about twice the matched values at each radius. The difference from the matched condition may be due to unmatched propagation of the beam or because high-energy or high-divergence shots

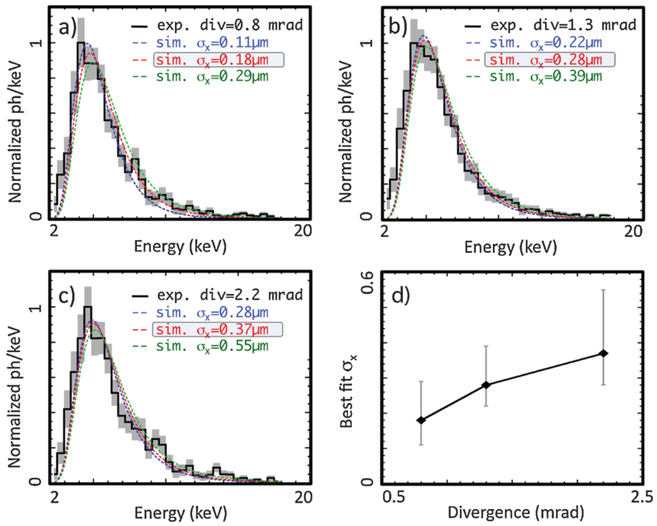

FIG. 3 (color). Binned detected x-ray betatron spectra (a)–(c) versus electron beam divergence. Shown are the detected spectrum (black; shaded region shows 1-σ uncertainty) and angle-integrated theoretical spectra, convolved with filters/detector response. The best fit is identified. Best fit σ_x versus divergence (d), with error bars at 95% confidence.

contribute disproportionately to the binned data, biasing binned fits to higher σ_x values.

Normalized transverse emittance was estimated using $\epsilon_x \approx \gamma\sigma_x\sigma_\theta$ to be $\sim$0.1 mm mrad for the shot in Fig. 2. Simulations [33,34] have indicated that particles trap transversely in the wake. It was previously observed [33] that the simulated σ_θ was lower, in closer agreement with experiments, in 3D simulations rather than in 2D, due to differing wake structure. Particles on injection trajectories can pass close to a spike in plasma density at the back of the bubble where fields are defocusing, reducing σ_x and σ_θ. In the present data both σ_x and σ_θ agree well with VORPAL [35] 3D particle-in-cell simulations, which observed $\sigma_{x(\mathrm{sim})} \sim 0.1$ μm rms and $\sigma_{\theta(\mathrm{sim})} \sim 1.3$ mrad rms at similar laser-plasma parameters and for electron bunches of 300 MeV with 2% rms energy spread and 1 fs rms length [33,36]. The present data extend the agreement between data and the physical picture observed in simulations to include σ_x and σ_θ. Such verification is important to the design and understanding of experiments. It indicates that self-trapping can result in transverse momenta well below those obtained from simple estimates of the bubble transverse potential. The trajectory and hence emittance will depend on the plasma wave amplitude and therefore on parameters including laser intensity and plasma density. This is consistent with the observed variation in the data and indicates that this process can be tuned to produce beams of controlled emittance. The observed emittance is similar to state of the art rf accelerators [37], though at lower charge.

In conclusion, measurements of single-shot, high-resolution x-ray spectra have been performed that demonstrate the synchrotron nature (i.e., continuum form) of the betatron emission from LPAs. Measurement of single-shot spectra in the range of 2–20 keV was enabled by using a CCD in photon-counting mode. Comparison of the measured spectra to analytical and numerical models of betatron radiation indicated the electron bunch radius inside the plasma to be $\sim$0.1 μm. In combination with divergence measurements, a normalized transverse emittance as low as 0.1 mm mrad was inferred for a 460 MeV, 2.8% rms energy-spread electron bunch of 0.4 pC charge. Reducing the beam emittance is necessary to enhance a variety of applications of relativistic electron beams, such as x-ray FELs, gamma sources, and colliders for high energy physics. The data agree with simulated bunch size and divergence, consistent with the simulated physical picture of self-trapping and emittance.

The authors thank the LOASIS team at LBNL as well as the VORPAL team at Tech-X and the Helmholtz Alliance HA216/EMMI. This work was supported by the Director, Office of Science, Office of High Energy Physics, U.S. Dept. of Energy under Contract No. DE-AC02-05CH11231, DOE NNSA NA-22, and NSF Grants No. PHY-0917687 and No. 0614001 and used the computational facilities at NERSC.

*Also at École Polytechnique, Palaiseau 91128, France.
†Also at GSI Helmholtzzentrum für Schwerionenforschung, D-64291 Darmstadt, Germany.
‡Also at SCIPP, University of California, Santa Cruz, CA 95064, USA.
§Also at University of California, Berkeley, CA, USA. wpleemans@lbl.gov.

[1] T. Tajima and J. M. Dawson, Phys. Rev. Lett. **43**, 267 (1979).
[2] E. Esarey, C. B. Schroeder, and W. P. Leemans , Rev. Mod. Phys. **81**, 1229 (2009).
[3] S. P. D. Mangles *et al.*, Nature (London) **431**, 535 (2004).
[4] C. G. R. Geddes, Cs. Toth, J. van Tilborg, E. Esarey, C. B. Schroeder, D. Bruhwiler, C. Nieter, J. Cary, and W. P. Leemans, Nature (London) **431**, 538 (2004).
[5] J. Faure, Y. Glinec, A. Pukhov, S. Kiselev, S. Gordienko, E. Lefebvre, J.-P. Rousseau, F. Burgy, and V. Malka, Nature (London) **431**, 541 (2004).
[6] W. P. Leemans, B. Nagler, A. J. Gonsalves, Cs. Tóth, K. Nakamura, C. G. R. Geddes, E. Esarey, C. B. Schroeder, and S. M. Hooker, Nature Phys. **2**, 696 (2006).
[7] W. P. Leemans *et al.*, Phys. Rev. Lett. **91**, 074802 (2003).
[8] J. van Tilborg, C. B. Schroeder, C. V. Filip, Cs. Tóth, C. G. R. Geddes, G. Fubiani, R. Huber, R. A. Kaindl, E. Esarey, and W. P. Leemans, Phys. Rev. Lett. **96**, 014801 (2006).
[9] A. Rousse *et al.*, Phys. Rev. Lett. **93**, 135005 (2004).
[10] K. T. Phuoc, F. Burgy, J.-P. Rousseau, V. Malka, A. Rousse, R. Shah, D. Umstadter, A. Pukhov, and S. Kiselev, Phys. Plasmas **12**, 023101 (2005).
[11] S. Kneip *et al.*, Nature Phys. **6**, 980 (2010).

[12] W. P. Leemans, D. Rodger, P. E. Catravas, C. G. R. Geddes, G. Fubiani, E. Esarey, B. A. Shadwick, R. Donahue, and A. Smith, Phys. Plasmas **8**, 2510 (2001).
[13] F. V. Hartemann, D. J. Gibson, W. J. Brown, A. Rousse, K. Ta Phuoc, V. Mallka, J. Faure, and A. Pukhov , Phys. Rev. ST Accel. Beams **10**, 011301 (2007).
[14] A. G. R. Thomas *et al.*, Phys. Rev. Lett. **98**, 095004 (2007).
[15] M. Fuchs *et al.*, Nature Phys. **5**, 826 (2009).
[16] H. P. Schlenvoigt *et al.*, Nature Phys. **4**, 130 (2008).
[17] J. Faure, C. Rechatin, A. Norlin, A. Lifschitz, Y. Glinec, and V. Malka, Nature (London) **444**, 737 (2006).
[18] K. Nakamura, B. Nagler, Cs. Tóth, C. G. R. Geddes, C. B. Schroeder, E. Esarey, W. P. Leemans, A. J. Gonsalves, and S. M. Hooker, Phys. Plasmas **14**, 056708 (2007).
[19] C. G. R. Geddes, K. Nakamura, G. R. Plateau, Cs. Toth, E. Cormier-Michel, E. Esarey, C. B. Schroeder, J. R. Cary, and W. P. Leemans, Phys. Rev. Lett. **100**, 215004 (2008).
[20] S. Fritzler, E. Lefebvre, V. Malka, F. Burgy, A. E. Dangor, K. Krushelnick, S. P. D. Mangles, Z. Najmudin, J.-P. Rousseau, and B. Walton, Phys. Rev. Lett. **92**, 165006 (2004).
[21] C. M. S. Sears, A. Buck, K. Schmid, J. Mikhailova, F. Krausz, and L. VeiszPhys. Rev. ST Accel. Beams **13**, 092803 (2010).
[22] E. Brunetti *et al.*, Phys. Rev. Lett. **105**, 215007 (2010).
[23] E. Esarey, B. A. Shadwick, P. Catravas, and W. P. Leemans, Phys. Rev. E **65**, 056505 (2002).
[24] I. Kostyukov, S. Kiselev, and A. Pukhov, Phys. Plasmas **10**, 4818 (2003).
[25] D. B. Thorn *et al.*, Rev. Sci. Instrum. **81**, 10E325 (2010).
[26] S. Fourmaux *et al.*, New J. Phys. **13**, 033017 (2011).
[27] F. Albert, R. Shah, K. Ta Phuoc, R. Fitour, F. Burgy, J.-P. Rousseau, A. Tafzi, D. Douillet, T. Lefrou, and A. Rousse , Phys. Rev. E **77**, 056402 (2008).
[28] K. Ta Phuoc, S. Corde, R. Shah, F. Albert, R. Fitour, J.-P. Rousseau, F. Burgy, B. Mercier, and A. Rousse , Phys. Rev. Lett. **97**, 225002 (2006).
[29] K. Nakamura, W. Wan, N. Ybarrolaza, D. Syversrud, J. Wallig, and W. P. Leemans, Rev. Sci. Instrum. **79**, 053301 (2008).
[30] G. R. Plateau *et al.*, Phys. Plasmas (unpublished).
[31] C. Fourment, N. Arazam, C. Bonte, T. Caillaud, D. Descamps, F. Dorchies, M. Harmand, S. Hulin, S. Petit, and J. J. Santos, Rev. Sci. Instrum. **80**, 083505 (2009).
[32] M. Chen *et al.* (unpublished).
[33] C. G. R. Geddes *et al.*, SciDAC Rev. **13**, 13 (2009).
[34] F. S. Tsung, R. Narang, W. B. Mori, C. Joshi, R. A. Fonseca, and L. O. Silva, Phys. Rev. Lett. **93**, 185002 (2004).
[35] C. Nieter and J. R. Cary, J. Comput. Phys. **196**, 448 (2004).
[36] C. G. R. Geddes *et al.*, J. Phys. Conf. Ser. **78**, 012021 (2007).
[37] Y. Ding *et al.*, Phys. Rev. Lett. **102**, 254801 (2009).